Kirschner, K., & Voigt, B. (1968) *Hoppe-Seyler's Z. Physiol. Chem. 349*, 632–644.
Klein, W. (1935) *Z. Physiol. Chem. 231*, 125–148.
Knivett, V. A. (1954) *Biochem. J. 56*, 606–610.
Koshland, D. E., Jr. (1952) *J. Am. Chem. Soc. 74*, 2286–2292.
Kresge, A. J., & Yang, Y. C. (1977) *J. Org. Chem. 42*, 757–759.
Lipmann, F., & Tuttle, L. C. (1947) *Arch. Biochem. Biophys. 13*, 373–377.
Long, J. W., & Ray, W. J., Jr. (1973) *Biochemistry 12*, 3932–3937.
Meunier, J.-C., & Dalziel, K. (1978) *Eur. J. Biochem. 82*, 483–492.
Needham, D. M., & Pillai, P. K. (1937) *Biochem. J. 31*, 1837–1851.
Negelein, E., & Brömel, H. (1939) *Biochem. Z. 303*, 132–114.
Negelein, E., & Brömel, H. (1969) in *Biological Phosphorylations* (Kalchar, H. M., Ed.) pp 102–114, Prentice-Hall, Englewood Cliffs, NJ.
Orsi, B. A., & Cleland, W. W. (1972) *Biochemistry 11*, 102–109.
Porter, W. R., & Trager, W. F. (1977) *Biochem. J. 161*, 293–302.
Pugh, W. (1929) *J. Chem. Soc.*, 1994–2001.
Richmond, T. G., Johnson, J. R., Edwards, J. O., & Rieger, P. H. (1977) *Aust. J. Chem. 30*, 1187–1194.
Sasaki, Y., Lindquist, I., & Sillen, L. G. (1959) *J. Inorg. Nucl. Chem. 9*, 93–94.
Schwarzenbach, G. (1958) *J. Inorg. Nucl. Chem. 8*, 302–312.
Segal, H. L., & Boyer, P. D. (1953) *J. Biol. Chem. 204*, 265–281.
Segel, I. H. (1975) *Enzyme Kinetics*, Wiley-Interscience, N.Y.
Seydoux, F. J., Kelemen, N., Kellershohn, N., & Roucous, C. (1976) *Eur. J. Biochem. 64*, 481–489.
Slocum, D. H., & Varner, J. E. (1960) *J. Biol. Chem. 235*, 492–495.
Storer, A. C., & Cornish-Bowden, A. (1974) *Biochem. J. 141*, 205–209.
Sutton, L. E., Ed. (1958) *Tables of Interatomic Distances and Configuration in Molecules and Ions*, No. 11, The Chemical Society, London.
Teipel, J., & Koshland, D. E., Jr. (1970) *Biochim. Biophys. Acta 198*, 183–191.
Travers, A., & Malaprade, L. (1926) *Bull. Soc. Chim. Fr. 39*, 1553–1573.
Trentham, D. R. (1971a) *Biochem. J. 122*, 59–69.
Trentham, D. R. (1971b) *Biochem. J. 122*, 71–77.
Velick, S. F., & Hayes, J. E., Jr. (1953) *J. Biol. Chem. 203*, 545–562.
Warburg, O., & Christian, W. (1939) *Biochem. Z. 303*, 40–68.
Winter, E. R. S., Carlton, M., & Brisco, H. V. A. (1940) *J. Chem. Soc.*, 131–138.

Relaxation Kinetics of Glutamate Dehydrogenase Self-Association by Pressure Perturbation†

Herbert R. Halvorson

ABSTRACT: The kinetics of self-association for beef liver glutamate dehydrogenase (EC 1.4.1.3) have been measured by using pressure perturbation in both the time domain and the frequency domain by monitoring scattered light intensity. The kinetic behavior is entirely consistent with the random self-association model proposed by Thusius et al. [Thusius, D., Dessen, P., & Jallon, J. M. (1975) *J. Mol. Biol. 92*, 413–432]. The activation volume $\Delta V^{\ddagger}$ for association is estimated to be positive, and it is shown that this provides further corroboration of the molecular mechanism advanced by these same authors. A rapid shift in scattered light intensity is attributed to preferential interaction between the phosphate anion and the protein, proceeding with a positive volume change (2–5 mL/mol of phosphate). A description of the instrument developed for this study is also included.

Beef liver glutamate dehydrogenase (EC 1.4.1.3) (GDH)[1] exists in solution as a molecule of 336 000 molecular weight, each molecule consisting of six apparently identical polypeptide chains. These molecules of GDH self-associate to form a concentration-dependent statistical distribution of rodlike aggregates, with a single equilibrium constant describing the addition of a unit to a growing chain. This phenomenon has been studied extensively and is covered in recent reviews devoted to GDH (Sund et al., 1975; Eisenberg et al., 1976). Although the mode of the interactions has been well characterized as a linear indefinite (or isodesmic) self-association by a variety of equilibrium techniques, equilibrium measurements, of course, leave the question of mechanism unresolved. For GDH self-association, it would be interesting to know if any particular oligomeric species plays a special role in the self-association process. The initial stopped-flow kinetic measurements (Fisher & Bard, 1969) showed uniphasic kinetics, suggesting the existence of but a single kinetic interaction. A more detailed temperature-jump study (Thusius et al., 1975) corroborates Fisher's observation and points out

† From the Department of Biochemistry and Molecular Biology, Edsel B. Ford Institute for Medical Research, Detroit, Michigan 48202. *Received November 21, 1978.* This work was supported by Grant GM 23302 from the National Institutes of Health and in part by an institutional grant to the Henry Ford Hospital from the Ford Foundation. The purchase of the digital signal averager was made possible by an equipment grant from the Ford Motor Company Fund.

[1] Abbreviations used: GDH, bovine liver glutamate dehydrogenase (EC 1.4.1.3).

0006-2960/79/0418-2480$01.00/0

the mechanistic implications of the way in which relaxation times vary with total protein concentration. The self-association equilibrium for GDH is consistent with two quite different kinetic schemes (Thusius, 1977): sequential indefinite self-association, in which growth of a chain proceeds solely by the addition of monomers, and random indefinite self-association, in which growth occurs by the combination of any oligomers. The random scheme predicts the observation of the single elementary relaxation. The sequential scheme predicts the occurrence of an infinite relaxation spectrum which, because of degeneracy and relative amplitudes, would be interpreted as a single relaxation. The way in which relaxation rates vary with total protein concentration supports the random indefinite self-association model. In dealing with such a polydisperse system one must make simplifying assumptions, and for the temperature-jump studies just mentioned, the assumptions pertain to the distribution of enthalpy changes among the interactions. Although the assumptions are reasonable, it is not inconceivable that a different distribution of the enthalpy changes and a different kinetic scheme might have led to the same observation. If there truly were heterogeneity in the interactions, it is unlikely that an independent thermodynamic property, volume, would be distributed in the same way as enthalpy. The pressure perturbation study reported here therefore provides strong substantiation for the random model. It also provides additional mechanistic information not revealed by other techniques.

The kinetics of protein self-association reactions have been studied previously by pressure-jump light-scattering experiments (Kegeles & Ke, 1975; Davis & Gutfreund, 1976; Tai et al., 1977; Kegeles, 1978). These experiments have entailed monitoring the exponential response to a single rapid compression or decompression of 100 atm or more. Because of the relative insensitivity of most chemical systems to pressure, the resulting perturbation of the equilibrium is comparable to that occurring in a typical temperature jump of 5 °C. For many systems this is a simple and direct way to obtain the desired kinetic information. In other cases, however, it may be desirable to avoid the elevated pressures and large jumps because of concerns about protein stability or a desire to produce only a minute perturbation of a very cooperative transition. Clegg et al. (1975) have used repetitive, small (less than 10 atm) pressure perturbations, with signal averaging techniques, to study order–disorder transitions in lipid vesicles and proteins. I have built a similar instrument and applied it to the self-association of GDH. Although the need for a small perturbation is not great in this particular case, the capability is important for study of other, more cooperative polymerizations such as those which are displayed by flagellin, myosin, actin, tubulin, or deoxyhemoglobin S.

Experimental Procedure

Materials. GDH was obtained from Sigma (type IV). After dialysis, solutions were clarified by centrifugation and used without further purification. Other chemicals were standard reagent grade. For all experiments reported here the buffer was 0.2 M potassium phosphate and 1 mM EDTA, pH 7.2. Concentration of GDH was determined spectrophotometrically [$A_{279}^{1\ mg/mL} = 0.97$ (Olson & Anfinsen, 1952)]. Light scattering was monitored at 400 nm.

Pressure Perturbation Instrument. The design of the instrument parallels that of the instrument developed by Clegg & Maxfield (1976) in its essential features. Figure 1 is a block diagram of the configuration for measurements in the frequency domain (dispersion). A pressure wave sinusoidal in time is generated by driving a stack of piezoelectric ceramics (LTZ-1, Transducer Products) with the high-voltage output of an operational power supply (OPS-2000, Kepco). The power supply in turn is driven by a variable-frequency, variable-phase function generator (HP-203A-001, Hewlett-Packard) which provides all the necessary timing information for the circuitry. The sample, contained in a short cylindrical optical cell (synthetic sapphire, Adolf Meller Co.) is illuminated with monochromatic light (H-20 holographic grating monochromator, Jobin-Yvon) from a 150 Xe arc (Osram) in an Oriel housing, powered by a constant-current power supply (XL 150, O.L.I.S.). Light scattered at 90° is detected with an EMI 9558QB end-on photomultiplier tube in a PPI 62/3A27 combination photomultiplier tube housing/photometer amplifier. Conversion to detection of fluorescence (emission filter) or transmittance (in-line observation) is simple. A reference photomultiplier tube samples the incident light, giving the capability of removing most of the lamp fluctuations. The difference between the two photomultiplier signals is taken with a Keithley 301 operational amplifier. A calibrated semiconductor bridge pressure transducer (XTM-1-190-500, Kulite Semiconductor Products, Inc.) monitors the pressure within the cell.

When the instrument is operated in the frequency domain, it employs fairly standard techniques of phase-sensitive detection and amplification in a homemade dual-channel device (Bentz et al., 1974; Mathis & Buck, 1976). Instead of the

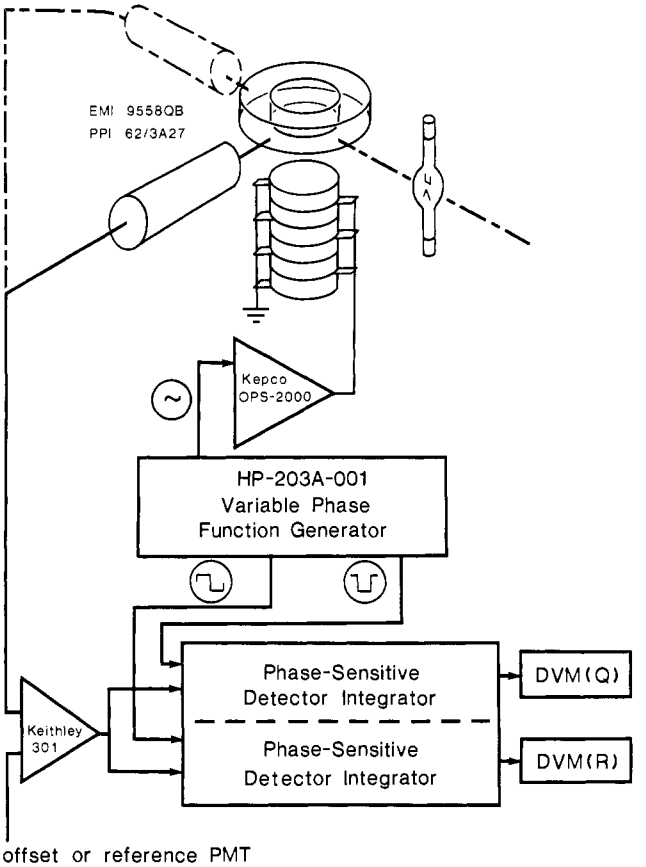

FIGURE 1: Block diagram of pressure relaxation instrument. Monochromatic light isolated from a Xe arc impinges on a short cylindrical cell. Alternate positions of the detector allow the monitoring of transmitted light or light emitted at 90°. Pressure is varied by driving a piezoelectric stack with the output of a programmable power supply. A variable-phase variable-frequency function generator synchronizes the pressure perturbation with the phase-sensitive detector/integrator. For time-domain experiments (not shown) the power supply is programmed with a square wave and the detector/integrator is replaced with a digital signal averager.

usual active filter, this circuit employs a gated integrator in the final stage. This approach obviates the attenuation of the signal to root mean square level and the difficulty of filtering out low-frequency ripple—two major problems with traditional lock-in techniques under these conditions (low signal and low frequency, respectively).

For kinetic measurements in the time domain, the piezoelectric stack is driven with a square wave, producing repetitive transient signals. The output of the Keithley 301 is then supplied to a digital signal averager (Tracor-Northern 507A), where successive transients are accumulated until a satisfactory ratio of signal to noise is achieved. The oscilloscope display is then photographed.

The enhancement of the ratio of signal to noise differs for the time domain and frequency domain techniques and is treated separately and more completely under Results. The extent to which random noise is reduced increases as the square root of the number of cycles. Sudden jumps in lamp intensity resulting from arc wander can be disastrous, but the differential measurement greatly reduces the influence of more minor (and more common) fluctuations. Smooth variations in lamp intensity (drift) will influence the total amplitude only, with no effect on rates or the fractional amplitudes of part processes.

The stainless steel bomb, which contains the piezoelectric stack, the optical cell, and the pressure sensor, was not thermostated in these experiments, although that capability now exists. Instead, its large thermal mass [7 kg, with a specific heat of 0.1 cal/(g deg)] was relied on to maintain the experimental temperature at room temperature (20 °C). Since the pressure-jump experiment is adiabatic rather than isothermal, it is appropriate to consider the validity of this assumption. Adiabatic heating of the sample is described by $(\partial T/\partial p)_S = \alpha T/\rho c_p$ which for water at 20 °C becomes 1.5×10^{-3} deg/atm. This effect is insufficient to sensibly perturb the chemical system and is canceled over each complete cycle. Cumulative electrical heating is diminished by the small power factor for the piezoelectric stack, which behaves like an almost pure capacitance. At 2 kV the dc current is less than 10^{-7} A, which for a 1-Hz square wave (50% duty cycle) is equivalent to about 10^{-5} cal/cycle. The net resistive heating over 2000 cycles would be less than 10^{-4} °C.

Theory. The principles of relaxation kinetics are familiar: by effecting a small perturbation of a chemical system at equilibrium, the rate at which the system relaxes to the new equilibrium conditions can be analyzed by using greatly simplified kinetic expressions (Eigen & de Maeyer, 1963, 1973; Bernasconi, 1976). The observed intensity can be expressed as

$$I_0 = HcM_w$$

where I_0 is the observed (static) intensity of scattered light, c is the mass concentration of macromolecule, M_w is the weight-average molecular weight of the solute, and H is the familiar "instrument constant"

$$H = 2\pi^2 n_0^2 (dn/dc)^2/(N_0 \lambda^4 r^2)$$

Since only small departures from I_0 are measured, it is legitimate to ignore the virial terms. The amplitude resulting from a small perturbation δp is given by

$$i = I_0(d \ln I_0/dp)\delta p$$

Measurements can be performed in the time domain (transient techniques) or the frequency domain (stationary techniques). Transient techniques ("jump" experiments) are characterized by an effectively instantaneous change in the perturbing variable, followed by an exponential decay in the observable to the new equilibrium. The stationary techniques (absorption or dispersion experiments) typically use a sinusoidally modulated perturbing variable, so the position of the equilibrium becomes a function of time. As the perturbation is swept or scanned from low to higher frequency, the observable signal is attenuated and shifted in phase. The relations are conveniently visualized in a phasor representation. Figure 2 illustrates a hypothetical pressure-modulation experiment on a self-associating system with a positive volume of association, by using scattered light as the observable. Each vector represents the amplitude and phase angle of a particular harmonic oscillation of angular frequency ω, with the real axis being defined by the perturbation. The physical response to the perturbation is effectively instantaneous and lies on the real axis. The signal depicted i_{phys} would pertain to an increase over the dc level due to the finite compressibility of the solvent. Changes in solvation producing changes in the refractive index increment would lead to positive or negative amplitudes for i_{phys}. The chemical response lags behind the perturbation by phase angle $\phi = \tan^{-1}(\omega\tau)$, the finite rate precluding instantaneous response. This "chemical compressibility" leads to a negative amplitude in the signal i_{chem} because a positive volume change means that an increase in pressure drives the system to lower M_w (less scattered intensity). The photomultiplier tube sees i_{signal}, the vector sum of i_{phys} and i_{chem}. Depending on the relative magnitude of i_{phys}, the apparent phase angle can deviate markedly from ϕ. Resolving i_{signal} into its two orthogonal components i_Q and i_R with phase-sensitive detection avoids this problem since i_Q contains no contribution from i_{phys}. The dashed line indicates the locus of i_{signal} as a function of frequency (Cole–Cole plot). When i_Q and i_R are displayed as functions of frequency (Figure 3), conventional dispersion curves result.

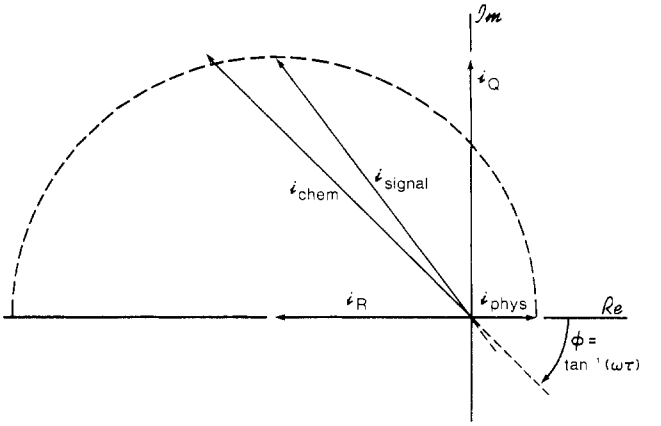

FIGURE 2: Phasor representation of frequency-domain pressure perturbation. The real axis is defined by the pressure perturbation. Physical response i_{phys} lies on the real axis, whereas chemical response i_{chem} is delayed by phase angle ϕ. The photomultiplier tube responds to i_{signal}, the vector sum of i_{phys} and i_{chem}. Phase-sensitive detection resolves i_{signal} into its two orthogonal components i_R and i_Q. The dashed line is the locus of i_{signal} as a function of frequency.

Analysis of experiments in the time domain generally follows the treatment developed for single transients. Particularly when dealing with slow relaxations, it can be advantageous to truncate the decay before it reaches the equilibrium value in order to collect more transients at the expense of decreased amplitude. The complete expression for the signal observed from a single normal relaxation[2] is

$$y = y^0\left(e^{-t/\tau}\frac{\tau}{\tau - \tau_p}\frac{1 - e^{-T/\tau_p}}{1 + e^{-T/\tau}} - e^{-t/\tau_p}\frac{\tau_p}{\tau - \tau_p}\right)$$

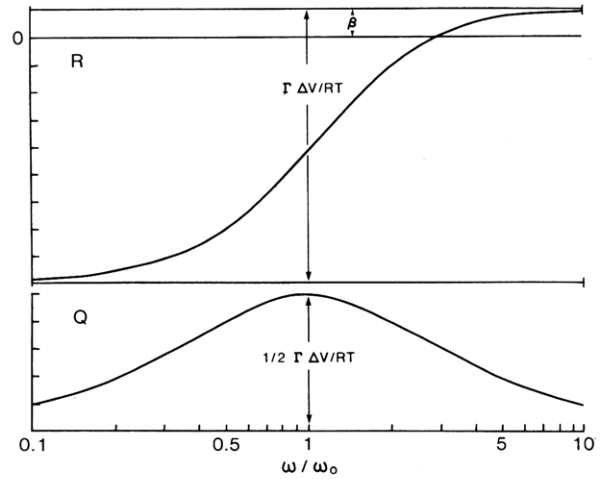

FIGURE 3: Dispersion curves for i_Q and i_R. The real component is given by $i_R = [\beta - (1 + \omega^2\tau^2)^{-1}\Gamma\Delta V/RT]\delta p$ and the quadrature or imaginary component by $i_Q = [\omega\tau(1 + \omega^2\tau^2)^{-1}\Gamma\Delta V/RT]\delta p$.

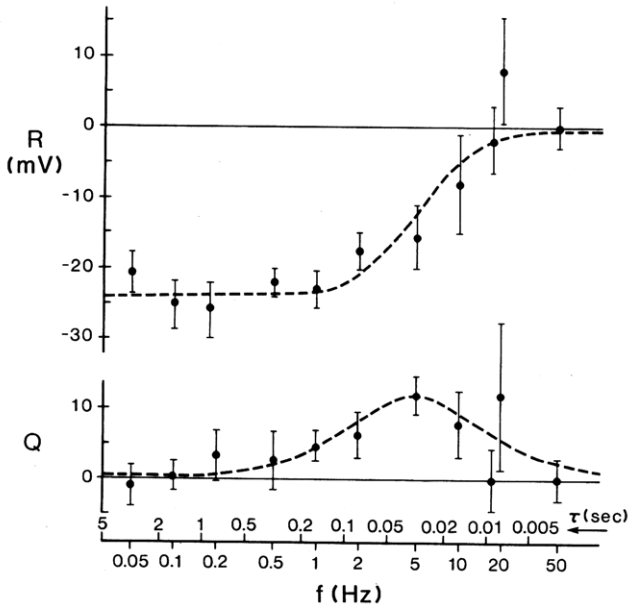

FIGURE 4: Relaxation of GDH (10 mg/mL) in the frequency domain. Points are the means (±SE) of 10 measurements. Solid lines are theoretical curves for a process with an amplitude of 24 mV and a relaxation time of 32 ms. See text for a discussion of data at 20 Hz.

where τ is the chemical relaxation time, τ_p is the time constant for the exponential change in pressure, and T is the duration of the perturbation (half the period of a square wave). These corrections for finite rise time and truncated decay were not required in the experiments reported here.

Results

Frequency Domain. A representative dispersion curve is shown in Figure 4. The theoretical curves were obtained by first defining the amplitude with a Cole–Cole type plot and then assigning the maximum in i_Q to $1/\tau$. This yields a relaxation time of 32 ms. The fit appears adequate, although least-squares treatment was not employed. The data at 20 Hz, not used in estimating τ, illustrate a point to be derived from Figure 5, which represents the relative discrimination of the amplifier/integrator. The signal entering this device contains noise components of many frequencies ω_i besides the component at the operating frequency Ω. The output voltage is derived by full-wave rectification (at frequency Ω), followed by integration over one complete cycle at the same frequency. The contribution of noise at frequency ω_i to the output voltage is expressed as

$$N_i = \int_0^{\Pi/\Omega} \sin(\omega_i t)\, dt - \int_{\Pi/\Omega}^{2\Pi/\Omega} \sin(\omega_i t)\, dt$$

and it is the absolute value of this function, normalized to unity at Ω, which is depicted in Figure 5. Not all noise frequencies are equally attenuated. When operating at 20 Hz, line frequency (60 Hz) is the first odd harmonic and it is not effectively removed. Accordingly, the values of i_Q and i_R at this frequency are strongly influenced by the phase relation between the pressure perturbation and the line voltage. The greatly increased uncertainties in the mean values at this frequency arise from a ratio of interference frequency to operating frequency which is not *exactly* 3. This produces beating. The data at 17.5 Hz (60/17.5 = 3.4) illustrate the ability of the analyzer to discriminate against a strong noise component under more favorable conditions. Although not shown here, even more striking effects are seen in the vicinity of 8 Hz, since the dominant noise frequency is 120 Hz (120/8 = 15). The presence of $1/f$ or flicker noise and the finite low-frequency

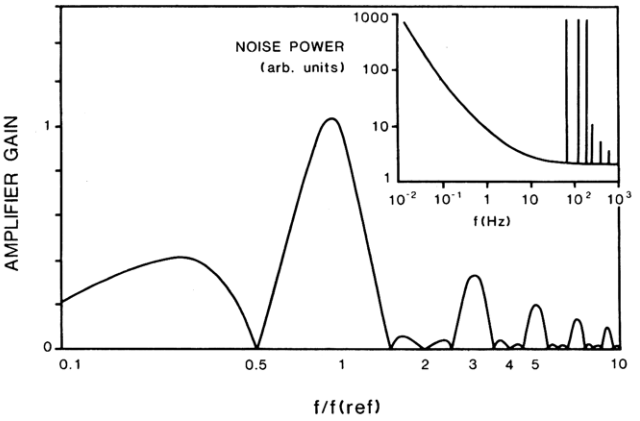

FIGURE 5: Response of phase-sensitive detector and gated integrator to inputs of differing ratios to the operating frequency. Inset: power spectrum of environmental noise showing $1/f$, interference, and "white" noise.

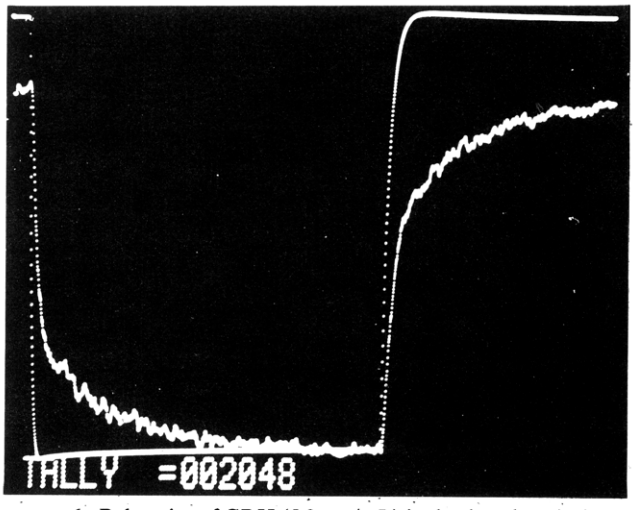

FIGURE 6: Relaxation of GDH (5.8 mg/mL) in the time domain (2048 transients). The optical signal is inverted by the difference amplifier, so the initial pressure drop (6 atm) produces an increase in the scattered intensity. The half-period of the square wave is 244 ms (f = 2.05 Hz). Amplitudes of the two traces are arbitrary.

[2] This corrects a minor typographical error in eq 15 of Clegg & Maxfield (1976).

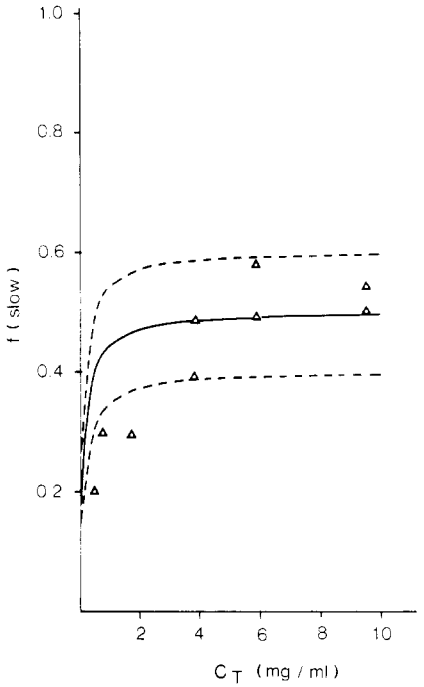

FIGURE 7: Fraction of the total change in optical signal due to the relaxation amplitude vs. total protein concentration. Points are experimental results, and lines are theoretical as described in the text.

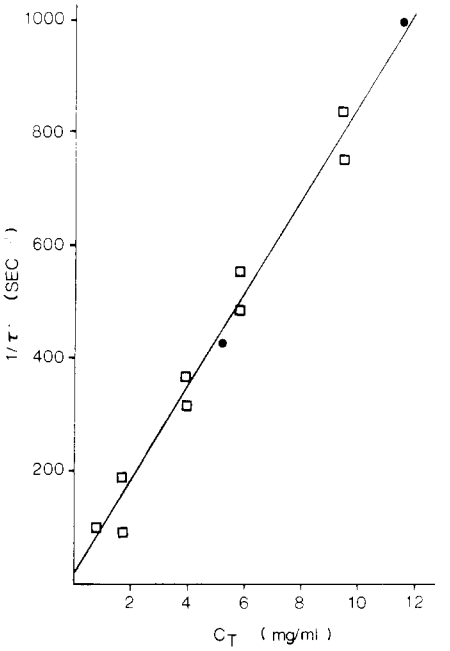

FIGURE 8: Reciprocal of the square of the relaxation time vs. total protein concentration. Experimental points are from measurements in the time domain (□) or frequency domain (●). Where relaxation times differ at the same concentration, the slower process always corresponds to the higher equilibrium pressure.

lobe for the analyzer response combine to preclude measurements much below 0.05 Hz. This is a general problem with techniques in the frequency domain, particularly when the ratio of signal to noise is low.

Time Domain. The results of a typical transient (time domain) experiment are shown in Figure 6. Although white (random) noise is suppressed as the square root of the number of repetitions, the relative contribution of interference noise will be enhanced if its frequency is a harmonic of the frequency of the square wave. These harmonics become closely spaced at low operating frequencies, leading to the appearance of "ringing" in the signal. Continued averaging of more transients cannot eliminate this from the record, so operating frequencies must be chosen carefully.

Another feature of the pressure-jump relaxation pattern is the presence of a fast process (following the time course of the perturbation, τ_p = 2 ms) with an amplitude of the same sign as the relaxation proper. Although this phenomenon was not noted in temperature-jump studies on this system (Thusius et al., 1975), similar effects have been seen in pressure-jump experiments with α-hemocyanin and attributed to changes in solvation involving larger volume changes than enthalpy changes (Tai et al., 1977). Preferential interaction of GDH with phosphate has been noted to increase the refractive index increment (Gauper et al., 1974). If this is the underlying cause of the fast process, then the preferential interaction between the two components proceeds with a net increase in volume. Such behavior would be consistent with removing the phosphate anion from "normal" aqueous solution to a region where less electrostriction would be obtained, i.e., in the immediate proximity of the protein molecule.

Relaxation curves were analyzed by plotting semilogarithmically points taken from the photographs and drawing a line through the points at longer times. "Curve peeling" was used to verify that the fast process occurred at the same rate as the perturbation. The fraction of the total amplitude caused by the slow phase was derived from the same plot. This information is presented in Figure 7.

Random indefinite self-association (Thusius et al., 1975; Thusius, 1977) can be regarded formally as a dimerization reaction between sites available for interaction, S, to form a bond or tight interaction, B,

$$2S \underset{k_d}{\overset{k_a/4}{\rightleftharpoons}} B$$

where the numerical factor arises from statistical considerations. As a consequence of this formal dimerization, the familiar transformation

$$(1/\tau)^2 = 4k_a k_d C_t + k_d^2$$

can be applied to test the concentration dependence of the experimentally observed rates and to derive the rate constants in the absence of ancillary information. The relaxation data are presented this way in Figure 8, which shows the equivalence of the time domain and frequency domain techniques. From the slope and intercept, I determine $k_a = 1.5 \times 10^6$ M^{-1} s^{-1} and $k_d = 5$ s^{-1}, equivalent to values determined earlier (Thusius et al., 1975).

Since each pressure-jump experiment gives two relaxations (at different pressures) and the rate at the higher pressure is consistently slower, the activation volume for self-association can be estimated from the pressure dependency of the rates. Differentiation of the expression for the relaxation time yields

$$\Delta V_a^{\ddagger} = \frac{1}{2}[1 + (\tau k_d)^2]\Delta V^{\circ} - RT\frac{\Delta \ln (1/\tau)}{\Delta p}$$

Under the conditions of these experiments the thermodynamic volume change for association is +24 mL/mol (Heremans, 1975) and k_d is 5 s^{-1}. The result, $\Delta V_a^{\ddagger} = +350 \pm 150$ mL/mol, presents immediate implications as to the nature of the transition state and the mechanism for the self-association process.

Discussion

The results obtained here on the kinetics of GDH self-association provide substantial corroboration for the random

indefinite associate model of Thusius et al. (1975). If the interactions in this system were truly heterogeneous, it would be quite unlikely that both ΔV and ΔH would be distributed so as to give an apparent single exponential decay (Figure 6) through degeneracy. The concentration dependence of the relaxation times shown in Figure 8 argues strongly against any special role for the monomer in the kinetic mechanism. Further insight into this system is provided by a closer consideration of the results in Figure 7 and 8.

Since the self-association occurs more slowly than a diffusion-controlled process yet the subunits must encounter one another in some diffusion-limited manner, it is helpful to consider a slightly more detailed kinetic scheme

$$2S \overset{1}{\rightleftharpoons} S_2 \overset{2}{\rightleftharpoons} B$$

where, as before, S represents a site available for interaction and B represents a bond or tight interaction. S_2 represents an encounter pair produced by the collision of two hydrated sites. Step 1 proceeds at a diffusion-limited rate, while the unimolecular conversion in step 2 is much slower, akin to the mechanism for ligand–metal complex formation (Eigen & Tamm, 1962). Since S and S_2 represent heterogeneous molecular populations, one cannot speak meaningfully of a single diffusion-controlled rate constant for step 1, but it is possible to estimate that the relaxation time for this step should not exceed 100 μs, which is significantly faster than the perturbation. Such a mechanism is consistent with all that is known about GDH self-association.

The fast relaxation process summarized in Figure 7 does not arise from step 1 of this mechanism, however, as can be shown by analyzing the amplitudes. Denoting by $\Delta\phi_i$ and ΔV_i the molar changes in light intensity and volume associated with each part reaction, the fraction of the total amplitude which occurs in the slow phase can be expressed (Schimmel, 1971; Thusius, 1972) as

$$f = [(\Delta\phi_1 - \Delta\phi_2) \times (\Delta V_1 - \Delta V_2) + \Delta\phi_2\Delta V_2 4K_1 s - \Delta\phi_1\Delta V_1 4K_1 s/(1 + 4K_1 s)]/[(\Delta\phi_1 - \Delta\phi_2)(\Delta V_1 - \Delta V_2) + \Delta\phi_2\Delta V_2 4K_1 s + \Delta\phi_1\Delta V_1/K_2]$$

where $s = (\sqrt{1 + 4K_1K_2C_t} - 1)/(K_1K_2)$ is the concentration of free sites. The $\Delta\phi$'s can be expressed as

$$\Delta\phi_1 = 2M_1^2[2H(S_2) - H(S)]$$

$$\Delta\phi_2 = 4M_1^2[H(B) - H(S_2)]$$

where allowance has been made for the "instrument constant" H (or, by implication, dn/dc) to be a function of the degree of association. Such a formulation is at odds with the well established idea that the dependence of light scattering on molecular size stems from interference effects in the solute particle and accordingly should be insensitive to the minute change implied for step 2. This implies that

$$\Delta\phi_1 = 4M_1^2H$$

$$\Delta\phi_2 = 0$$

leading to

$$f = \frac{1 - \frac{\Delta V_1}{\Delta V_2}\frac{1}{1 + 4K_1 s}}{1 - \frac{\Delta V_1}{\Delta V_2}\left(1 + \frac{1}{K_2}\right)}$$

The nature of the two steps implies that $\Delta V_1 \ll \Delta V_2$ and f becomes indistinguishable from 1. This is not in accord with the results shown in Figure 7.

Compressibility of the solvent can be immediately rejected as an explanation because it would produce a jump opposite in sign to the relaxation amplitude. A remaining plausible explanation is a decrease of refractive index increment with increasing pressure. Since scattered intensity varies as the square of the refractive index increment, the amplitude expected is

$$\delta I = -2I_0 D\delta p$$

where $D = -\partial \ln (dn/dc)/\partial p$. The relaxation proper will have an amplitude (Thusius et al., 1975) of

$$\delta I = -I_0\frac{2KC_t}{M_1 + 4KC_t}\frac{\Delta V}{RT}\delta p$$

The fraction of the amplitude occurring in the slow phase is then

$$f = \frac{\frac{1}{D}\frac{\Delta V}{RT}\frac{K}{M_1}C_t}{1 + \left(4 + \frac{1}{D}\frac{\Delta V}{RT}\right)\frac{K}{M_1}C_t}$$

This expression is plotted in Figure 7 for different limiting values of f, and from the solid line it appears that an appropriate estimate is 0.5 or $D = 2.5 \times 10^{-4}$.

Preferential interaction of GDH with phosphate has been noted previously (Gauper et al., 1974) through the effect of phosphate concentration on the refractive index increment of the protein. Analyzing their data through the procedures described by Casassa & Eisenberg (1964) leads to an estimate of 180 ± 5 mol of phosphate per mol of GDH in 0.5 M phosphate buffer, pH 6.5. (This represents 30 mol of phosphate per polypeptide chain, in reasonable accord with 26 mol of NaCl per mol of BSA under similar conditions.) Using the empirical formulas of Teller (1976) for the accessible surfaces of proteins, the fraction of the surface which is occupied by phosphate (0.03) does not differ materially from the estimated volume fraction of phosphate in the solution (0.05). Indirect support for the idea that these are nonspecific interactions comes from the relative insensitivity of the self-association to the phosphate concentration, d ln K/d ln (phosphate) = –0.92 at 10 °C, pH 6.5 (Gauper et al., 1974), suggesting that only a negligible fraction of the bound phosphate is linked to the self-association, perhaps involving specific interactions. (The kinetic uncoupling of the two processes is established by the experiments reported here.) It is then reasonable to suppose that these are weak, nonspecific interactions involving one RT (0.6 kcal) of excess free energy for each phosphate (Schellman, 1978). In the absence of a specific binding isotherm, the thermodynamic measure of binding reduces to

$$\frac{\partial m_3}{\partial m_2} = \mu_2(\text{excess})/RT$$

by using the Scatchard formalism (Casassa & Eisenberg, 1964). Assumption of this linear free energy model, ignoring the 0.7 change in pH, leads to an estimate of 72 mol of phosphate per mol of GDH for the preferential interaction under the conditions of these experiments. At this lower phosphate concentration the excess refractive index increment is predicted to be 0.0040 mL/g. For a 6-atm perturbation, the change found experimentally (-2.9×10^{-4} mL/g) is 7.2% of this, leading to an estimated ΔV of +3.8 mL/mol of

phosphate. If the limiting values of f are taken to be 0.4 or 0.6 (dashed lines of Figure 7), the corresponding estimates of ΔV become +5.6 or +2.5 mL/mol, respectively. Overall, an estimate of +2–6 mL/mol seems appropriate. Although the total amount of phosphate bound and the associated change in refractive index increment are estimated with uncertainty, the estimate of the volume change associated with binding one phosphate is robust with respect to such error.

The source of this volume increase could lie in either or both of two processes. As the phosphate ion and the protein molecule become associated, some of their hydration shells could be shared, and the resulting release of bound water would increase the thermodynamic volume of the system. This would involve perhaps 2–6 water molecules per phosphate ion. Alternatively, there should be some neutralization of charge as the phosphate ion is brought from bulk solvent to the more nonpolar milieu in the immediate vicinity of the protein surface. The volume changes suggest 10–25% of the effect associated with removal of one formal charge. There are important subtleties in considering preferential interaction. Foremost is recognizing that the interaction is described in terms of components of the solution, that is, entities whose concentration can be independently varied, not in terms of ion binding. To avoid playing too freely with this important distinction, it is useful to consider "phosphate" as representing a hypothetical molecule whose properties reflect the mole fraction of total phosphate which is K_2HPO_4 or KH_2PO_4. For example, from molar and ionic volumes tabulated by Millero (1972), it is possible to estimate molar volumes of 25.7 and 38.1 mL/mol, respectively, for these two species. At pH 7.2 and 0.2 M, the phosphate component has a "molar volume" of 28.8 mL/mol. Assigning the volume change for the preferential interaction to the phosphate component means that the "bound phosphate" has a "molar volume" of 32.6 mL/mol. This represents a distribution of species that, at 0.2 M total phosphate, has a pH of 6.6. Another way of viewing the situation, perhaps more illuminating, is that the phosphate component in bulk solution is best described as $K_{1.75}H_{1.25}PO_4$, whereas in the vicinity of the protein, it behaves more like $K_{1.44}H_{1.56}PO_4$, and it is in this way that we are seeing the volume of ionization for phosphate and electrostrictive effects. The net effect is to bring protons to the protein. This description is simplistic in its neglect of the charge on the protein, about which little can be said other than that the sign is negative at this pH.

A temperature jump of 5 °C would produce about the same change in the refractive index increment (Gauper et al., 1974), but the amplitude of the relaxation proper would be 25–30 times greater, making it difficult or impossible to see the fast process (Thusius et al., 1975). Alternative explanations might be sought in the decrease in pH (~0.002) induced by a 6-atm increase in pressure, although this would imply an unusually strong dependence of preferential interaction or solvent refractive index upon pH. The similar effects observed by Kegeles and co-workers (Tai & Kegeles, 1971; Tai et al., 1977) occurred with α-hemocyanin in acetate buffer, ruling out behavior unique to phosphate (or GDH) as an explanation. Their proportionately smaller fast process would be consistent with the smaller volume of ionization for acetate, but no quantitative conclusion can be drawn from the single relaxation curve (Figure 2 of Tai et al., 1977).

It is unsatisfying to have no better direct evidence for this proposed explanation, particularly when considering the relatively poor agreement at low concentration. Three factors conspire against a more stringent test by varying the phosphate concentration. First, the predominant effect of the resulting change in the refractive index increment will be to change each amplitude proportionally. Second, the self-association equilibrium depends on ionic strength, leading to changes of the slow amplitude with salt concentration. Third, preferential interactions are far weaker than stoichiometric binding (the molar ratio of phosphate to GDH is approximately 50 000), making it difficult to alter significantly the extent of perturbation. The instability of GDH in other buffers, such as Tris, precludes study in such media. Detailed studies of the effect of pH and ionic strength on the kinetics (now in progress) will help to clarify the picture.

The unusually large activation volume is readily interpreted with the aid of a simple model for the transition state between the encounter pair, S_2, and the formed interaction, B. If the encounter pair involves the collision of the hydration layers and the interaction requires the approximation of the protein surfaces, then the intervening water molecules must leave that region before the proteins can move together. Each water molecule so implicated contributes its molar volume (18 mL/mol) to the activation volume, and it appears[3] that some 20 water molecules play such a kinetic role. Thusius et al. (1975) have suggested, from considerations of the entropy changes, that 24 water molecules are released in the association equilibrium. From the effect of pressure on the self-association equilibrium (Heremans, 1975), one can likewise infer the involvement of 25–30 water molecules. The smaller number found from the kinetic experiments may be an insignificant difference, although it is more likely that the dissolution of the hydration shell is not a totally concerted process. The previously determined activation parameters (Thusius et al., 1975) then become $\Delta H^{\ddagger} = 0.75$ kcal/mol, $\Delta S^{\ddagger} = 1$ cal/(mol deg), and $\Delta C_p^{\ddagger} = 15$ cal/(mol deg) for each water molecule. In the absence of structural information about the interface, these parameters cannot be sensibly dissected further to describe the hydration of nonpolar vs. polar groups.

Pressure perturbation relaxation studies are seen to provide unique information on macromolecular interactions as well as to corroborate conclusions drawn independently via other techniques. Volumes of reaction are every bit as ubiquitous as heats of reaction, so most processes can be perturbed directly. When the direct volume change is vanishingly small, the reaction of interest can be coupled with a rapid responsive reaction to provide the requisite kinetic information, as is commonly done in temperature-jump studies. When optical detection is used, there are almost no constraints on solvent composition (ionic strength, for example).

An additional advantage of this instrument, also pointed out by Clegg et al. (1975), arises from the use of small perturbations, despite the ensuing difficulty in measuring the small signals. A key feature in the popularization of relaxation techniques is that rate equations of any order can be linearized for a sufficiently small perturbation of the equilibrium. When dealing with highly cooperative systems, particularly those with high apparent molecular order, the allowable perturbation becomes quite small (Bernasconi, 1976). The problems involved in measuring the resulting small signals are obvious and

[3] In this context it must be mentioned that, although the experimental estimate of $\Delta V^{\ddagger}$ is significantly different from 0 at the 0.95 level by the t test, the 0.95 confidence interval for $\Delta V^{\ddagger}$ is 350 ± 430 mL/mol. Accordingly, the conservative interpretation of these results is that only the sign of $\Delta V^{\ddagger}$ has been determined. Arguments based on the magnitude of $\Delta V^{\ddagger}$ must be regarded as tentative until more precise estimates become available. What is at question is not the general validity of the simple model presented but rather the degree to which the expulsion of the hydration layer is a concerted process.

pressure perturbation lends itself well to the required signal averaging techniques. Perhaps less obvious is the ease with which very small perturbations can be applied. For GDH with ΔV = 25 mL/mol and ΔH = 5 kcal/mol, a 1.0-atm pressure jump is equivalent to a temperature jump of 0.03 °C. The pressure-volume work of 25 (mL atm)/mol would perturb the free energy by 0.6 cal/mol, and the experiment would approach the realm of fluctuation kinetics.

Despite the attractive features of techniques in the frequency domain (simplicity and economy of instrumentation and analysis), this approach does not prove sufficiently powerful for studying systems with small signals and slow relaxations. It may be more valuable in studying other kinds of interactions.

Added in Proof

Information recently obtained from Dr. K. A. Heremans (personal communication) suggests that ΔV^* is about +10 mL/mol. His estimate (to be published in detail elsewhere) derives from experiments specifically designed to measure this parameter (temperature jump at 1–600 atm) and must be regarded as being more precise than that obtained in this work. The mechanistic implication is that surface water molecules are displaced more or less independently.

Acknowledgments

Conversations with Drs. R. M. Clegg, E. L. Elson, K. A. Heremans, G. Kegeles, and B. W. Maxfield have been very helpful in diverse aspects of this work.

References

Bentz, A. J., Sandifer, J. R., & Buck, R. P. (1974) *Anal. Chem. 46*, 543–547.
Bernasconi, C. F. (1976) *Relaxation Kinetics*, p 76, Academic Press, New York.
Casassa, E. F., & Eisenberg, H. (1964) *Adv. Protein Chem. 19*, 287–395.
Clegg, R. M., & Maxfield, B. W. (1976) *Rev. Sci. Instrum. 47*, 1383–1393.
Clegg, R. M., Elson, E. L., & Maxfield, B. W. (1975) *Biopolymers 14*, 883–887.
Davis, J. S., & Gutfreund, H. (1976) *FEBS Lett. 72*, 199–207.
Eigen, M., & Tamm, K. (1962) *Ber. Bunsenges. Phys. Chem. 66*, 93–121.
Eigen, M., & de Maeyer, L. (1963) *Tech. Org. Chem. 8 (part 2)*, 895–1054.
Eigen, M., & de Maeyer, L. (1973) *Tech. Chem. (N.Y.) 6 (part 2)*, 63–146.
Eisenberg, H., Josephs, R., & Reisler, E. (1976) *Adv. Protein Chem. 30*, 101–181.
Fisher, H. F., & Bard, J. R. (1969) *Biochim. Biophys. Acta 188*, 168–170.
Gauper, F. P., Markau, K., & Sund, H. (1974) *Eur. J. Biochem. 49*, 555–563.
Heremans, K. A. H. (1975) *Rev. Phys. Chem. Jpn. 1975s*, 627–630.
Kegeles, G. (1978) *Methods Enzymol. 48*, 308–320.
Kegeles, G., & Ke, C. (1975) *Anal. Biochem. 68*, 138–147.
Mathis, D. E., & Buck, R. P. (1976) *Anal. Chem. 48*, 2033–2035.
Millero, F. J. (1972) in *Water and Aqueous Solutions* (Horne, R. A., Ed.) pp 519–595, Wiley-Interscience, New York.
Olson, J. A., & Anfinsen, C. B. (1952) *J. Biol. Chem. 197*, 67–69.
Schellman, J. A. (1978) *Biopolymers 17*, 1305–1322.
Schimmel, P. R. (1971) *J. Chem. Phys. 54*, 4136–4137.
Sund, H., Markau, K., & Koberstein, R. (1975) *Biol. Macromol. 7C*, 225–287.
Tai, M. S., & Kegeles, G. (1971) *Arch. Biochem. Biophys. 142*, 258–267.
Tai, M. S., Kegeles, G., & Huang, C. (1977) *Arch. Biochem. Biophys. 180*, 537–542.
Teller, D. C. (1976) *Nature (London) 260*, 729–731.
Thusius, D. (1972) *J. Am. Chem. Soc. 94*, 356–363.
Thusius, D. (1977) *Mol. Biol., Biochem. Biophys. 24*, 339–370.
Thusius, D., Dessen, P., & Jallon, J. M. (1975) *J. Mol. Biol. 92*, 413–432.

Ion Binding to Cytochrome *c* Studied by Nuclear Magnetic Quadrupole Relaxation†

Thomas Andersson,* Eva Thulin, and Sture Forsén*

ABSTRACT: The enhancement of the $^{35}Cl^-$ transverse relaxation rate on binding of chloride ions to oxidized and reduced cytochrome *c* has been studied under conditions of variable sodium chloride concentration, temperature, pH, sodium phosphate, iron hexacyanide, and sodium cyanide concentration. The results revealed the presence of a strong binding site(s) for chloride in both oxidized and reduced cyt *c*, with a higher affinity in ferrocytochrome *c*. Competition experiments suggest that these sites also bind iron hexacyanide and phosphate. Cyanide binding to the iron in ferricytochrome *c* at alkaline and neutral pH was shown to decrease the binding of chloride. The pH dependence of the $^{35}Cl^-$ relaxation rate has been fitted by using literature p*K* values for ionizable groups. No indications of Na^+ binding to oxidized and reduced cytochrome *c* have been observed by using $^{23}Na^+$ NMR. Our results suggest that chloride is bound near the exposed heme edge and that the surface structure or dynamics in this region are different in the two oxidation states.

Eucaryotic cytochrome *c* is a small protein, composed of 103–113 amino acid residues, having an iron porphyrin covalently attached to the protein. The biological role of cytochrome *c* is to receive electrons from cytochrome c_1 and in turn deliver them to cytochrome oxidase (Dickerson & Timkovich, 1975). The crystal structure of tuna cytochrome *c* has been determined for both oxidation states (Swanson et al., 1977; Takano et al., 1977; Mandel et al., 1977), and no

† From the Department of Physical Chemistry 2, University of Lund, Chemical Center, S-220 07 Lund, Sweden. *Received November 22, 1978.* First presented, in part, at the European Conference on NMR of Macromolecules, Sassari, Sardinia, May 1978.

0006-2960/79/0418-2487$01.00/0